

DiverseDream: Diverse Text-to-3D Synthesis with Augmented Text Embedding

Uy Dieu Tran^{1*} Minh Luu^{1*} Phong Nguyen² Janne Heikkilä² Khoi Nguyen¹ Binh-Son Hua³
¹VinAI Research, Vietnam ²University of Oulu, Finland ³Trinity College Dublin, Ireland

Abstract

Text-to-3D synthesis has recently emerged as a new approach to sampling 3D models by adopting pretrained text-to-image models as guiding visual priors. An intriguing but underexplored problem with existing text-to-3D methods is that 3D models obtained from the sampling-by-optimization procedure tend to have mode collapses, and hence poor diversity in their results. In this paper, we provide an analysis and identify potential causes of such a limited diversity, and then devise a new method that considers the joint generation of different 3D models from the same text prompt, where we propose to use augmented text prompts via textual inversion of reference images to diversify the joint generation. We show that our method leads to improved diversity in text-to-3D synthesis qualitatively and quantitatively.

1. Introduction

The realm of 3D content creation has persistently posed intricate challenges within the domains of computer vision and computer graphics. Over time, various methodologies have emerged to address this challenge. Traditional techniques in generating 3D models often necessitate user interaction, involving meticulous shaping of scene geometry and appearance through software like Blender [2]. Another prevalent avenue revolves around scene reconstruction using multi-view geometry principles, extensively explored in literature such as [25]. These approaches have garnered substantial adoption, particularly within industries like interior design and computer animation, revolutionizing their workflows and creative possibilities.

The rise of deep learning has led to increased interest in developing data-driven techniques to automate 3D modeling. Several efforts have been made to generate 3D models by learning directly from 3D data [43]. However, due to the scarce availability of 3D data, it has been of great interest to explore the generation of 3D data by learning from different modalities such as images and natural languages. It has been shown that pretrained text-to-image diffusion models can serve as a strong prior to guiding the optimization of a 3D

model represented by a neural radiance field in DreamFusion with SDS loss [33], from which text-to-3D synthesis emerges as a promising research direction.

While text-to-3D synthesis has shown interesting results, an intriguing issue is that the generated 3D models remain limited in several aspects including fidelity, diversity, optimization convergence, and scalability. Some efforts have been made to address these problems, ranging from an improved loss function in ProlificDreamer [47], amortized generation over different text prompts in ATT3D [27], to personalized generation in DreamBooth3D [35]. Among these leading efforts to improve text-to-3D synthesis, diversity has been an underexplored aspect, and there is little insight into how diversity is achieved in existing text-to-3D methods.

In this paper, we investigate the diversity of 3D model generation from state-of-the-art text-to-3D methods. We argue that the diversity is affected by the objective function such as SDS [33] and VSD [47] given a text prompt to condition the 3D model generation. Inspired by this observation, we propose to diversify text-to-3D generation results by applying an augmentation to the original text prompt in the text embedding via textual inversion techniques [12, 15]. Our idea is to first sample reference images from a pretrained text-to-image diffusion model and then find the corresponding text features of these images. By using these augmented text features to condition the optimization process to sample 3D models instead of the original text prompt, we show that the diversity of the 3D models can be significantly improved. Our experiments show that our method outperforms the state-of-the-art text-to-3D methods in terms of diversity quantitatively and qualitatively.

In summary, our contributions are:

- An empirical analysis of the diversity of existing text-to-3D methods;
- A general technique based on augmented text embedding acquired from textual inversion of 2D reference images to improve the diversity and speed of the optimization process;
- Extensive experiments and ablation studies that demonstrate the validity and robustness of our method, which is applicable to different text-to-3D methods;

*First two authors contribute equally.



A brightly colored mushroom growing on a log



A cocktail



A glowing lantern



A 3D model of an adorable cottage with a thatched roof



A small saguaro cactus planted in a clay pot



A birthday cake rendered in 3D

Figure 1. We address the intriguing low-diversity issue in text-to-3D synthesis by reconsidering the text prompt used by variational score distillation [47]. We propose to use reference images to sample augmented text prompts via textual inversion and use these augmented text prompts to condition the particles in the variational inference of text-to-3D optimization to learn more diverse 3D representations. Thanks to the diversity in the reference images (top-left inline images), we obtain diverse 3D models that inherit certain structures from their references.

2. Related Work

Text-to-image synthesis has witnessed tremendous growth in the past years. The first group of methods [3, 19, 41] are built upon Generative Adversarial Networks (GANs), which leverage an actor-critic loss for training their image generators. Despite the capability of GANs to generate fast and realistic images, they are susceptible to mode collapse. An alternative group of approaches is auto-regressive models, for example, DALL-E [36], Parti [52], and MUSE [6] which model the generation of an image patch based on another one, resulting in a sequential generation modeling. A recent notable family of text-to-image synthesis is based on diffusion models, such as Stable Diffusion [38], DALL-E 3 [42], and Imagen[40], which have demonstrated great potential to synthesize high-resolution high-quality images. In this paper, we resort to diffusion-based models, e.g., Stable Diffusion, as the pretrained 2D prior for supervising our 3D model generation.

3D representation is the core of generative 3D models for various 3D tasks, such as novel view synthesis and 3D content creation. Neural Radiance Fields (NeRFs) [29], distinguished for its utilization of volumetric rendering, has gained considerable attraction in learning a 3D scene representation under solely 2D image supervision. Despite NeRF’s pervasive application [46] in both 3D reconstruction and generation domains, its optimization process has been identified as time-intensive [13]. There is a vast amount of work addressing the speed convergence issue and improving view synthesis performance using hybrid neural scene representations such as voxel grids [44, 51], hash-grid [30], tri-planes [4, 7] and Gaussian splatting [21]. Among those hybrid scene representations, hash-grids [30] has been extensively used for the text-to-3D task [33, 47] due to its fast training, superior performance compared to vanilla NeRFs, and absence of bias phenomena observed in the tri-planes. This paper also utilizes hash grids to learn a set of diverse 3D scene representations from a single text prompt via our proposed textual score distillation loss.

Image-to-3D generation is an important direction of conditional generative 3D models. Early work on single view synthesis [31, 49] leverages a differentiable neural renderer to warp the input view and then refine it to perform novel view synthesis. However, such approaches are limited by the distance between the input and target pose and it is not trivial to produce a full 360° reconstruction given a single input. There has been significant progress with the emerging generative models. Zero-1-to-3 [25] pioneers open-world single-image-to-3D conversion through zero-shot novel view synthesis. However, the geometric inconsistency in its generated images has yet to bridge the gap between multi-view images and 3D scenes. Recent works such as One-2-3-45

[24], SyncDreamer [26], and Consistent123 [48] build extra geometry-constraint layers upon Zero-1-to-3 to obtain more 3D-consistent results. However, training image-to-3D models usually requires 3D model datasets such as ShapeNet [5], CO3D [37], or large-scale multiview datasets such as Objaverse [10] or Objaverse-XL [9]. Our approach, on the other hand, is only based on a pretrained text-to-image model for supervision, which is more accessible.

Text-to-3D generation. Recent advances in this topic have demonstrated outstanding potential for generating complex 3D models based solely on 2D priors by utilizing pre-trained text-to-image models such as Stable Diffusion [38]. DreamField [18] is a notable early work in this field that employs CLIP [34] to minimize the disparities between the rendered image and the input text across a predetermined set of random perspectives. However, the quality of 3D models generated by DreamField is often compromised due to the limited ability of the CLIP model to capture the rendered image’s semantic features fully. In response to this limitation, DreamFusion [33] proposes a substitution of the CLIP loss with the Score Distillation Sampling (SDS) loss and introduces an efficient method for calculating the gradients to learn a neural radiance field for 3D synthesis. Unfortunately, DreamFusion tends to generate objects with oversmooth surfaces and saturated colors. Several subsequent methods aim to improve upon DreamFusion in many directions: higher resolution [23], richer appearance [8], faster speed [45], photorealistic appearance [20, 47], single view [11, 28, 50]. Despite such rapid development, limited efforts have been spent to investigate the diversity aspect of text-to-3D synthesis, which motivates our work.

Textual inversion. Recent text-to-image diffusion models [38, 42] manage to render high-quality 2D images, but they can not guarantee to preserve the shape and identity of the subject or “personalization”. There exist inversion methods to maintain the identity of the subject in the reference images such as Textual Inversion [12] and DreamBooth [39]. They introduce a virtual token whose corresponding embedding can be optimized and manipulate the generated 2D images. Based on Textual Inversion, HiPer inversion [15] further enhances the inversion capability by using only one reference image and storing the object identity in some optimized textual tokens of the text prompt. This key observation motivates us to apply textual inversion to diversify the generated 3D content.

3. Background

A typical approach to text-to-3D synthesis is to leverage the 2D prior from a pretrained text-to-image model such as Stable Diffusion (SD) [38], to guide the training of a 3D model represented by a neural radiance field (NeRF). In particular, a NeRF parameterized by θ is optimized so that

its rendered images $x = g(\theta, c)$, with g as the volumetric rendering function and c as the camera pose, look realistic and conform to the text prompt y .

Score distillation sampling (SDS): DreamFusion [33] introduced the SDS loss whose gradient is computed as:

$$\nabla_{\theta} \mathcal{L}_{\text{SDS}} = \mathbb{E}_{t, \epsilon, c} \left[\omega(t) (\epsilon_{\text{SD}}(x_t, t, y) - \epsilon) \frac{\partial g(\theta, c)}{\partial \theta} \right], \quad (1)$$

where $\omega(t)$ is a time-dependent weighting function, ϵ_{SD} is the predicted noise of SD given the noisy input image $x_t = \alpha_t x + \sigma_t \epsilon$ created by adding Gaussian noise ϵ to the rendered image x at timestep t with noise scheduling coefficients α_t, σ_t . However, the SDS loss often suffers from over-saturation, over-smoothing, and low-diversity issues as empirically analyzed in [47].

The particular issue of low diversity in SDS can be empirically observed in that the optimization from different runs tends to give similar results.

Therefore, we advocate the use of the more sophisticated variational score distillation loss [47] for our exploration of the diversity of text-to-3D synthesis, which we briefly describe below.

Variational score distillation (VSD): ProlificDreamer [47] addresses the aforementioned limitations of DreamFusion by proposing a variational form of score distillation. Their VSD loss attempts to address the low-diversity issue by modeling the distribution of 3D model output from a single text prompt as $\mu(\theta|y)$. Note that SDS is a special case of VSD, when $\mu(\theta|y)$ reduces to a Dirac distribution $\delta(\theta - \theta^1)$, having only a single 3D representation θ^1 for each text prompt.

To optimize VSD, the distribution μ is approximated by K learnable particles where each particle i corresponds to a 3D representation parameterized by θ_i which is sampled from a set of K particles $\{\theta_i\}_{i=1}^K$ for each training iteration, following the particle-based variational inference framework. The gradient of the VSD loss is as follows:

$$\nabla_{\theta_i} \mathcal{L}_{\text{VSD}} \triangleq \mathbb{E}_{t, \epsilon, c} \left[\omega(t) (\epsilon_{\text{SD}}(x_t^i, t, y) - \epsilon_{\phi}(x_t^i, t, c, y)) \frac{\partial g(\theta_i, c)}{\partial \theta_i} \right], \quad (2)$$

where ϵ_{ϕ} is a fine-tuned version of the original SD using the LoRA [17] parameterization ϕ on the rendered images of in-progress learning NeRFs. LoRA can be regarded as the *domain adaptation* of SD to noisy images rendered from NeRFs since SD is not originally trained on noisy images. Specifically, ϕ is trained with the following objective:

$$\min_{\phi} \mathbb{E}_{t, \epsilon, c} \left[\|\omega(t) (\epsilon_{\phi}(x_t, t, c, y) - \epsilon)\|_2^2 \right]. \quad (3)$$

Beyond its theoretical modeling of 3D representations as a distribution, an empirical observation on why the VSD

Algorithm 1 Algorithm of DiverseDream.

Input: K particles, K reference images $\{x_i^r\}_{i=1}^K$ from prompt y , pretrained text-to-image model ϵ_{SD} .

Stage 1: HiPer tokens inversion

- 1: **initialize** K HiPer tokens $\{h_i\}_{i=1}^K$.
- 2: **for** $i=1$ **to** K **do**
- 3: Optimize h_i given x_i^r following Eq. (4) to obtain h_i^* .
- 4: **end for**
- 5: **return** optimized $\{h_i^*\}_{i=1}^K$

Stage 2: Textual score distillation

- 1: **initialize** K NeRFs $\{\theta_i\}_{i=1}^K$, shared learnable tokens ϕ .
 - 2: **while** not converged **do**
 - 3: Sample noise ϵ , camera pose c , timestep t , and index i , obtain θ_i , and form text prompt $y'_i = [y; h_i^*; \phi]$.
 - 4: Render image $x_i = g(\theta_i, c)$ from NeRF θ_i at pose c , and compute x_i^i .
 - 5: Update θ_i following Eq. (6).
 - 6: Update ϕ following Eq. (7).
 - 7: **end while**
 - 8: **return** optimized $\{\theta_i^*\}_{i=1}^K$
-

loss enhances the diversity compared to the SDS loss is that the objective of VSD for each particle is different from each other. Notably, the second term $\epsilon_{\phi}(x_t^i, t, c, y)$ (in Eq. (2)) dynamically changes due to the learning progression of ϕ and the input image x_t^i rendered from the current particle θ_i .

Although the VSD loss addressed the limitation of SDS loss and clearly improved the quality of the 3D representations, we empirically found that it still yields limited diversity in some particular prompts. To further improve diversity, we propose to use augmented text embedding guided by 2D reference images, which is presented in the next section.

4. Our Approach

Inspired by textual inversion methods [12, 15] for 2D object personalization, we aim to condition text-to-3D synthesis such that the per-particle difference in $\epsilon_{\phi}(x_t^i, t, c, y'_i)$ is boosted by using different and distinct prompt y'_i for each particle θ_i .

Particularly, we consider the distribution of 3D representations from a given text prompt y . Our goal is to diversify the sampling for this distribution so that the sampled representations align with the given text prompt while having significant differences in terms of geometry and/or appearance. Our key idea is to diversify the 3D representations by diversifying their language descriptions. We observe that an object can be described in multiple valid ways, implying the existence of various text prompts that correspond to the input prompt y . By sampling these valid text prompts, denoted as $y'_i \sim p(y'|y)$, we can distill the 3D models using these prompts, thereby introducing diversity into the model. To

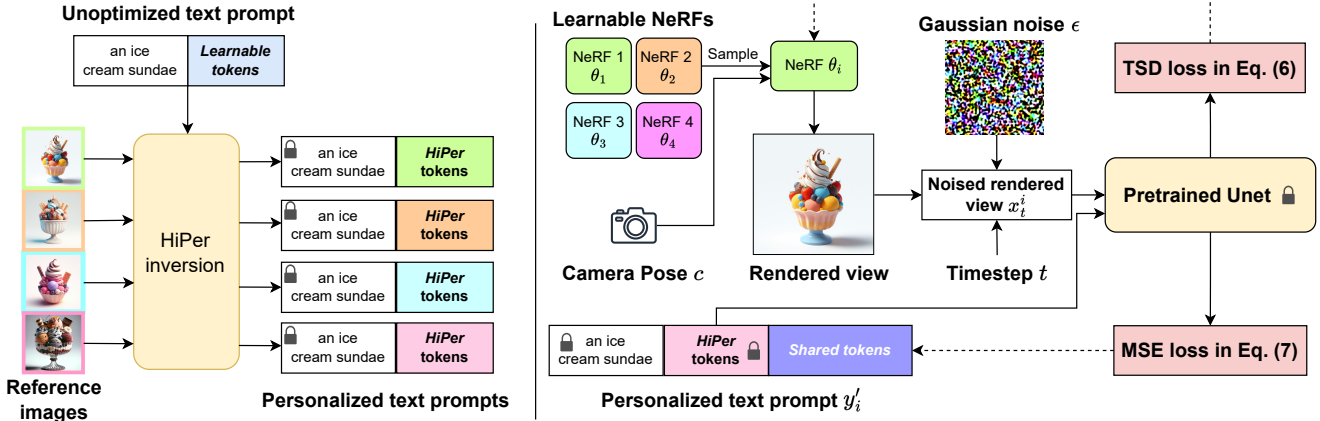


Figure 2. We translate the diversity of augmented text prompts to the resulting 3D models via a two-stage method. **Stage 1: HiPer tokens inversion** (left): for each reference image, we seek to learn a HiPer token h_i so that the prompt $[y; h_i]$ reconstructs the reference image. **Stage 2: Textual score distillation** (right): we run a multi-particle variational inference for optimizing the 3D models from text prompt y . For each iteration in the optimization, we randomly sample a particle θ_i with its rendered image x_i . We use the augmented text prompt $y'_i = [y; h_i^*; \phi]$, with ϕ as shared embedding to condition the optimization of θ_i (Eq. (6) and Eq. (7)).

this end, we devise a new approach that leverages HiPer textual inversion [15] to enhance the resulting diversity.

Overview. Our method has two stages: HiPer tokens inversion and textual score distillation. In the first stage, we sample a reference image x_i^r for each particle and find an optimized HiPer token h_i^* so that the reference image can be faithfully reconstructed by the pretrained text-to-image diffusion model with the prompt $[y; h_i^*]$, where $[\cdot; \cdot]$ is the concatenation operation. In the second stage, multiple particles θ_i are jointly optimized along with a new shared domain adaptor ϕ which is also encoded as a learnable token to form the augmented text prompt $[y; h_i^*; \phi]$ for each particle. The algorithm is shown in Alg. 1.

4.1. HiPer tokens inversion

We first sample K reference images $\{x_i^r\}_{i=1}^K$ corresponding to K particles from any text-to-image model given text prompt y . We empirically find that using Stable Diffusion (SD) [38] with additional guidance like “X with white background” gives the most suitable images for HiPer textual inversion. This is because we only have one image for inversion and we want to exclude noisy factors like background, facilitating faster and better textual inversion.

Subsequently, we want to optimize HiPer tokens for each reference image using the technique in [15]. Specifically, given a reference image x_i^r and a text prompt $y \in \mathbb{R}^{L_1 \times D}$ with L_1 as the number of text tokens and D as feature dimensions, we seek to find HiPer tokens $h \in \mathbb{R}^{L_2 \times D}$ with L_2 as the number of HiPer tokens to reflect the personalized identity of the object in x_i^r . To this end, we append the learnable tokens h_i to the original text prompt y to form new text personalized text prompt $y_i = [y; h_i] \in \mathbb{R}^{(L_1+L_2) \times D}$, and

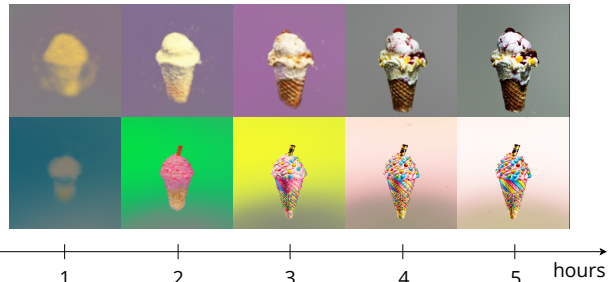


Figure 3. Optimization progression of VSD (upper) vs ours (lower). TSD with less # learnable parameters ϕ converges faster than VSD.

use HiPer [15] to optimize h_i with the objective:

$$\min_{h_i} \mathbb{E}_{t, \epsilon} [\|\omega(t) \epsilon_{\text{SD}}(x_{t,i}^r, t, [y; h_i]) - \epsilon\|_2^2]. \quad (4)$$

Note that HiPer use Stable Diffusion (version 1.4) for textual inversion. This stage is visualized in Fig. 2 (Left). The optimized h_i^* is leveraged as the key component to diversify the results of text-to-3D synthesis in the next step.

4.2. Textual score distillation (TSD)

With the learned personalized text prompts $y_i = [y; h_i^*]$, we are ready to use them to replace the original text prompt y in any text-to-3D approaches such as ProlificDreamer [47] to enhance the diversity of these approaches. However, we discover that the Domain Adaptor ϕ in ProlificDreamer, which is implemented using LoRA [17], can be further replaced by the textual inversion technique like HiPer [15]. This is similar to the problem of 2D object personalization where LoRA Dreambooth [39] can be replaced by Textual Inversion [12] or HiPer [15] with similar performance. The observation motivates us to devise a new Domain Adaptor $\phi \in \mathbb{R}^{L_3 \times D}$

in the form of shared learnable tokens in the text prompt among particles. That is, the new personalized text prompt:

$$y'_i = [y; h_i^*; \phi] \in \mathbb{R}^{(L_1+L_2+L_3) \times D}, \quad (5)$$

where L_3 is the number of shared learnable tokens. The new text prompt y'_i can replace the LoRA implementation ϕ of ProlificDreamer, resulting in the following Textual Score Distillation (TSD):

$$\begin{aligned} \nabla_{\theta_i} \mathcal{L}_{\text{TSD}} \triangleq & \quad (6) \\ \mathbb{E}_{t, \epsilon, c} \left[\omega(t) (\epsilon_{\text{SD}}(x_t^i, t, y_i) - \epsilon_{\text{SD}}(x_t^i, t, y'_i)) \frac{\partial g(\theta_i, c)}{\partial \theta_i} \right]. \end{aligned}$$

Compared to the LoRA implementation, the term $\epsilon_{\text{SD}}(x_t^i, t, y'_i)$ with shared learnable tokens has the advantage of faster training speed since the number of our learnable parameters ϕ (about 30K parameters) is much smaller than those of LoRA (about 1.3M parameters). The training of the shared learnable tokens is similar to the LoRA implementation, i.e., via a separate updating step from the updating step of each particle as:

$$\min_{\phi} \mathbb{E}_{t, \epsilon, c} [\|\omega(t)(\epsilon_{\text{SD}}(x_t, t, y'_i) - \epsilon)\|_2^2]. \quad (7)$$

In Fig. 2 (Right), we show how we train the sampled NeRF model θ_i and shared token ϕ using the proposed TSD (equation 6) and MSE (equation 7) losses respectively. As can be seen in the Fig. 3, our method can produce higher quality samples than those produced by VSD [47] given the same amount of optimization time.

5. Experiments

Metrics. The common metrics for generative models such as FID [16] do not separately measure fidelity and diversity. Inspired by [1], we proposed to use a modified version of *Inception Quality (IQ)* and *Inception Variance (IV)* to measure the quality and diversity of our models. Our IQ and IV are formulated as follows:

$$\text{IQ}(\theta) = \mathbb{E}_{i, c} [\mathcal{H}[p(y | x_i = g(\theta_i, c))]], \quad (8)$$

$$\text{IV}(\theta) = \mathcal{H}[\mathbb{E}_{i, c}[p(y | x_i = g(\theta_i, c))]], \quad (9)$$

where $p(y | x_i = g(\theta_i, c))$ is the pretrained classifier given the rendered images x_i from particles i . The entropy \mathcal{H} serves as an indicator of the classifier’s confidence when presented with an input-rendered image. The IQ metric captures the expected entropy, reflecting the classifier’s certainty across all views, which indicates the image quality to some degree (*the lower the better*). Conversely, the IV metric quantifies the entropy of the expected classifier outputs (*the higher the better*). A higher IV score is achieved when the classifier outputs are uniformly distributed, indicating

	IQ ↓	IV ↑	Cosine Sim ↓
SDS [33]	3.4692	4.2915	0.7465
VSD [47]	3.1716	4.2734	0.5383
TSD (ours)	3.5132	4.7181	0.5024

Table 1. Quantitative comparison with SOTA methods.

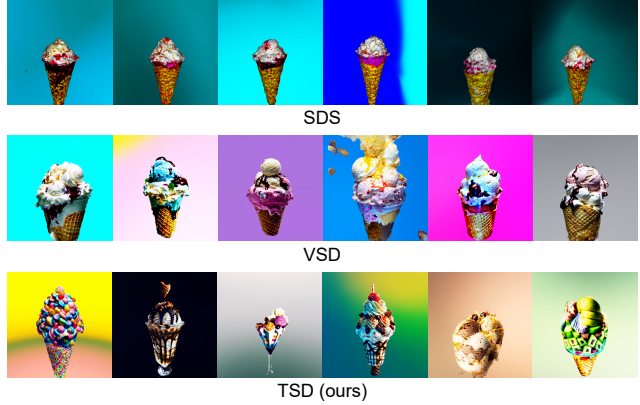


Figure 4. Diversity comparison between SOTAs and our method.

greater diversity in the input images. We rendered 120 views for each particle to compute IQ and IV.

We also propose the *Cosine Sim* metric to quantify the diversity of our particles. Specifically, for a given set of K particles, we render the same view for each particle. The rendered images are then fed through a feature extractor (e.g., as DINO [53]) to obtain feature vectors. We then calculate the cosine similarity for these feature vectors across $\binom{K}{2}$ pairs and take the average. To ensure robustness, we also average the results over 120 rendered views.

Implementation details. Our method is implemented with threestudio, an open-source framework for text-to-3D synthesis [14]. We use $K = 6$ particles for both VSD and our framework, TSD. The training of all experiments is conducted for 50K iterations. We use $L_2 = 5$ as HiPer tokens optimized in 1.4K iterations. Also, we use $L_3 = 8$ as shared learnable tokens ϕ and trained in 50K iterations. For the camera embedding, we use the same implementation as threestudio [14]. Regarding the resolution, we train each particle at 256×256 for all methods. We will release our code upon publication.

Baselines. We compare our method with two prominent text-to-3D methods including DreamFusion [33] and ProlificDreamer [47]. Note that we do not compare to other variants such as Magic3D [23] or Fantasia3D [8] since these methods address different issues of SDS, which is orthogonal to our method which focuses on diversity. For validation, we select a set of 10 text prompts from DreamFusion [33] and 10 text prompts generated randomly from ChatGPT [32].

ϵ_ϕ	HiPer	IQ ↓	IV ↑	Cosine Sim ↓	Training time
LoRA	No	3.1716	4.2734	0.5383	10.23
LoRA	Yes	3.4661	4.7462	0.4726	9.50
Shared tokens	Yes	3.5132	4.7181	0.5024	7.16

Table 2. Ablation study of our method.

# HiPer tokens	IQ ↓	IV ↑	Cosine Sim ↓
1	4.1406	5.4939	0.5526
5	4.2611	5.4653	0.5580
10	3.7975	5.2350	0.4554
15	4.2976	5.9625	0.3531
20	4.4228	5.8485	0.3983

Table 3. Ablation study on the number of HiPer tokens.

5.1. Comparison with SOTA

Quantitative comparison. We present our quantitative results in Tab. 1. It is evident that we outperform VSD and SDS in terms of IV Score and Cosine Sim, which measure the diversity between the particles. The IQ score of our method is slightly lower than VSD, which demonstrates there remains some fidelity-diversity trade-off, which is well known for existing text-to-image methods. Our method outperforms SDS in both diversity and quality.

Qualitative comparison. The comparative results in Fig. 4 demonstrate that our method offers more diversity among particles compared to VSD and SDS. For example, when given “A high-quality ice cream sundae” prompts, VSD tends to collapse into cone-shaped ice cream, while our method is capable of generating glass shapes and other variants.

Furthermore, we observe that our generated 3D models inherit the texture and structure of the reference image, as depicted in Fig. 1. This indicates the potential of transferring the diversity of 2D to 3D through text prompt augmentation. It is worth noting that we do not require the HiPer framework to perfectly invert the reference images, we only need HiPer tokens to capture the essence of reference images to ensure the diversity among personalized text prompts.

5.2. Ablation Study

Number of HiPer tokens L_2 . We vary the number of the HiPer tokens from 1, 5, 10, 15, and 20 using the prompt “Michelangelo style statue of a dog reading news on a cell-phone”, Fig. 5 and Tab. 3 show that while altering token length has a subtle impact on the 3D model, the text-to-image model produces images more closely resembling the reference in 2D.

LoRA vs. shared learnable tokens. We further validate the effect of our shared learnable tokens. When replacing the LoRA layer with our learnable tokens, our method can still achieve diverse results compared to SDS and VSD, although the quality was not as good as our method with LoRA, as

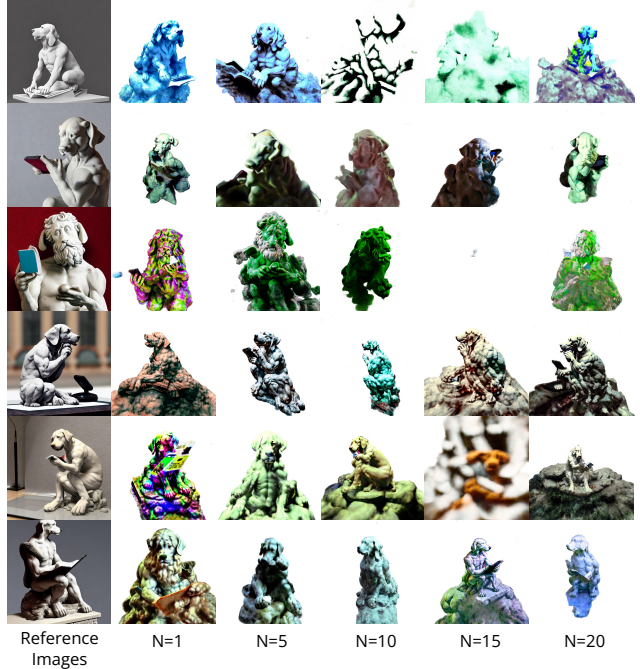


Figure 5. Visual results with different numbers of HiPer tokens.

shown in Tab. 2. However, the advantage of using shared learnable tokens is that it achieves a better training speed compared to the use of LoRA.

Comparison to LLM-based text prompt augmentation.

In addition to personalized text prompts obtained by image-to-text inversion using HiPer [15] as presented in the main paper, here we provide a comparison to a different text prompt sampling technique where the augmented text prompts are generated using large language models (LLMs) from an original text prompt. Particularly, given a text prompt y , we use ChatGPT [32] to generate K prompts from y with more details added to describe the object in y . For example, with an original prompt of “A high-quality photo of an ice cream sundae”, we can obtain an augmented text prompt of “A high-quality photo of an ice cream sundae with fresh berries and mint leaves”. We then follow our method in using the i -th prompts to condition the i -th particle in the VSD loss, respectively. The results are shown in Fig. 6. Compared to our method, LLM-based augmented text prompts also lead to diverse 3D generations, but their quality and diversity remain inferior compared to our image-to-text inversion.

5.3. User Study

We conducted a user study to evaluate the fidelity and diversity of the results obtained by our method and Prolific-Dreamer [47]. Our survey displays 23 prompts with results of models A and B, where participants are asked to select a model (A or B) that has better quality and diversity in terms of object shape and appearance. Models A and B are shuffled in each question to prevent users from biasing toward a single



Figure 6. Comparison between our HiPer inversion with LLM-generated augmentation for text prompt sampling. It can be seen that the use of reference images in our method leads to better fidelity and diversity.

	Quality	Diversity
VSD [47]	39.61%	39.90%
TSD (ours)	60.39%	60.10%

Table 4. User study on the fidelity and diversity of our method compared to ProlificDreamer [47].

selection. For each prompt, four video results for each model are displayed in each row. We distributed the survey to users from various backgrounds, including university students, researchers, and general PC/laptop/mobile phone users. In total, we received responses from 52 participants. After checking all responses and filtering out incomplete/invalid responses, there remains a total of 45 participants with 1035 responses. The results of the survey in Tab. 4 show that our method is better in terms of fidelity and diversity than VSD [47], with more than 60% of the responses favoring our results.

6. Discussion

Limitations. First, despite our model’s ability to enhance the diversity of the existing VSD framework, it still has some limitations. Our models heavily depend on the capacity of

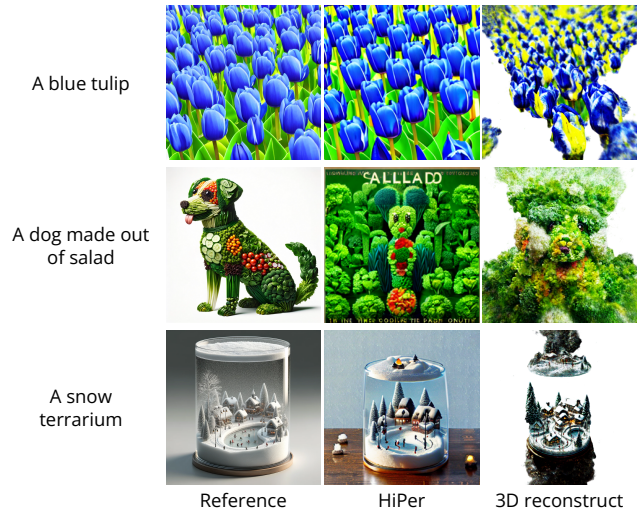


Figure 7. Failure cases due to the quality of reference images and capacity of HiPer tokens.

the HiPer inversion model [15], and if the reference image is an outlier of what the pretrained diffusion model can generate, HiPer may struggle to accurately invert it, resulting

in 3D models with weird shape and appearance. Some failure cases are shown in Fig. 7. Second, as our method is based on VSD, we share its limitations such as the Janus problem. Orthogonal methods that mitigate the Janus problem for VSD should be applicable to our method as well.

Conclusion. In this paper, we have successfully introduced a new text-to-3D synthesis method that focuses on diversifying the 3D generation by using 2D reference images and textual inversion to build augmented text prompts for conditioning the optimization. In future work, we plan to experiment with our augmented text embedding technique for other text-to-3D methods [8, 22], and more 3D representations [21].

References

- [1] Anonymous. Taming mode collapse in score distillation for text-to-3d generation. In *Submitted to The Twelfth International Conference on Learning Representations*, 2023. under review. 6
- [2] Blender Online Community. *Blender - a 3D modelling and rendering package*. Blender Foundation, Blender Institute, Amsterdam, 2018. 1
- [3] Andrew Brock, Jeff Donahue, and Karen Simonyan. Large scale GAN training for high fidelity natural image synthesis. In *International Conference on Learning Representations*, 2019. 3
- [4] Eric R Chan, Connor Z Lin, Matthew A Chan, Koki Nagano, Boxiao Pan, Shalini De Mello, Orazio Gallo, Leonidas J Guibas, Jonathan Tremblay, Sameh Khamis, et al. Efficient geometry-aware 3d generative adversarial networks. In *Proceedings of the IEEE/CVF Conference on Computer Vision and Pattern Recognition*, pages 16123–16133, 2022. 3
- [5] Angel X Chang, Thomas Funkhouser, Leonidas Guibas, Pat Hanrahan, Qixing Huang, Zimo Li, Silvio Savarese, Manolis Savva, Shuran Song, Hao Su, et al. Shapenet: An information-rich 3d model repository. *arXiv preprint arXiv:1512.03012*, 2015. 3
- [6] Huiwen Chang, Han Zhang, Jarred Barber, AJ Maschinot, Jose Lezama, Lu Jiang, Ming-Hsuan Yang, Kevin Murphy, William T Freeman, Michael Rubinstein, et al. Muse: Text-to-image generation via masked generative transformers. *arXiv preprint arXiv:2301.00704*, 2023. 3
- [7] Anpei Chen, Zexiang Xu, Andreas Geiger, Jingyi Yu, and Hao Su. Tensorf: Tensorial radiance fields. In *European Conference on Computer Vision (ECCV)*, 2022. 3
- [8] Rui Chen, Yongwei Chen, Ningxin Jiao, and Kui Jia. Fantasia3d: Disentangling geometry and appearance for high-quality text-to-3d content creation. In *Proceedings of the IEEE/CVF International Conference on Computer Vision (ICCV)*, 2023. 3, 6, 9
- [9] Matt Deitke, Ruoshi Liu, Matthew Wallingford, Huong Ngo, Oscar Michel, Aditya Kusupati, Alan Fan, Christian Laforte, Vikram Voleti, Samir Yitzhak Gadre, Eli VanderBilt, Aniruddha Kembhavi, Carl Vondrick, Georgia Gkioxari, Kiana Ehsani, Ludwig Schmidt, and Ali Farhadi. Objaverse-xl: A universe of 10m+ 3d objects. *arXiv preprint arXiv:2307.05663*, 2023. 3
- [10] Matt Deitke, Dustin Schwenk, Jordi Salvador, Luca Weihs, Oscar Michel, Eli VanderBilt, Ludwig Schmidt, Kiana Ehsani, Aniruddha Kembhavi, and Ali Farhadi. Objaverse: A universe of annotated 3d objects. In *Proceedings of the IEEE/CVF Conference on Computer Vision and Pattern Recognition*, pages 13142–13153, 2023. 3
- [11] Congyue Deng, Chiyu “Max” Jiang, Charles R. Qi, Xinchun Yan, Yin Zhou, Leonidas Guibas, and Dragomir Anguelov. Nerdi: Single-view nerf synthesis with language-guided diffusion as general image priors. In *Proceedings of the IEEE/CVF Conference on Computer Vision and Pattern Recognition (CVPR)*, pages 20637–20647, 2023. 3
- [12] Rinon Gal, Yuval Alaluf, Yuval Atzmon, Or Patashnik, Amit Haim Bermano, Gal Chechik, and Daniel Cohen-or. An image is worth one word: Personalizing text-to-image generation using textual inversion. In *The Eleventh International Conference on Learning Representations*, 2023. 1, 3, 4, 5
- [13] Stephan J Garbin, Marek Kowalski, Matthew Johnson, Jamie Shotton, and Julien Valentin. Fastnerf: High-fidelity neural rendering at 200fps. In *Proceedings of the IEEE/CVF International Conference on Computer Vision*, pages 14346–14355, 2021. 3
- [14] Yuan-Chen Guo, Ying-Tian Liu, Ruizhi Shao, Christian Laforte, Vikram Voleti, Guan Luo, Chia-Hao Chen, Zi-Xin Zou, Chen Wang, Yan-Pei Cao, and Song-Hai Zhang. three-studio: A unified framework for 3d content generation, 2023. 6
- [15] Inhwa Han, Serin Yang, Taesung Kwon, and Jong Chul Ye. Highly personalized text embedding for image manipulation by stable diffusion. *arXiv preprint arXiv:2303.08767*, 2023. 1, 3, 4, 5, 7, 8
- [16] Martin Heusel, Hubert Ramsauer, Thomas Unterthiner, Bernhard Nessler, and Sepp Hochreiter. Gans trained by a two time-scale update rule converge to a local nash equilibrium. In *Advances in Neural Information Processing Systems*. Curran Associates, Inc., 2017. 6
- [17] Edward J Hu, Yelong Shen, Phillip Wallis, Zeyuan Allen-Zhu, Yuanzhi Li, Shean Wang, Lu Wang, and Weizhu Chen. LoRA: Low-rank adaptation of large language models. In *International Conference on Learning Representations*, 2022. 4, 5
- [18] Ajay Jain, Ben Mildenhall, Jonathan T Barron, Pieter Abbeel, and Ben Poole. Zero-shot text-guided object generation with dream fields. In *Proceedings of the IEEE/CVF Conference on Computer Vision and Pattern Recognition*, pages 867–876, 2022. 3
- [19] Minguk Kang, Jun-Yan Zhu, Richard Zhang, Jaesik Park, Eli Shechtman, Sylvain Paris, and Taesung Park. Scaling up gans for text-to-image synthesis. In *Proceedings of the IEEE Conference on Computer Vision and Pattern Recognition (CVPR)*, 2023. 3
- [20] Oren Katzir, Or Patashnik, Daniel Cohen-Or, and Dani Lischinski. Noise-free score distillation. *arXiv preprint arXiv:2310.17590*, 2023. 3
- [21] Bernhard Kerbl, Georgios Kopanas, Thomas Leimkühler, and George Drettakis. 3d gaussian splatting for real-time radiance

- field rendering. *ACM Transactions on Graphics*, 42(4), 2023. 3, 9
- [22] Chen-Hsuan Lin, Jun Gao, Luming Tang, Towaki Takikawa, Xiao-hui Zeng, Xun Huang, Karsten Kreis, Sanja Fidler, Ming-Yu Liu, and Tsung-Yi Lin. Magic3d: High-resolution text-to-3d content creation. In *IEEE Conference on Computer Vision and Pattern Recognition (CVPR)*, 2023. 9
- [23] Chen-Hsuan Lin, Jun Gao, Luming Tang, Towaki Takikawa, Xiao-hui Zeng, Xun Huang, Karsten Kreis, Sanja Fidler, Ming-Yu Liu, and Tsung-Yi Lin. Magic3d: High-resolution text-to-3d content creation. In *IEEE Conference on Computer Vision and Pattern Recognition (CVPR)*, 2023. 3, 6
- [24] Minghua Liu, Chao Xu, Haian Jin, Linghao Chen, Zexiang Xu, Hao Su, et al. One-2-3-45: Any single image to 3d mesh in 45 seconds without per-shape optimization. *arXiv preprint arXiv:2306.16928*, 2023. 3
- [25] Ruoshi Liu, Rundi Wu, Basile Van Hoorick, Pavel Tokmakov, Sergey Zakharov, and Carl Vondrick. Zero-1-to-3: Zero-shot one image to 3d object. In *Proceedings of the IEEE/CVF International Conference on Computer Vision (ICCV)*, pages 9298–9309, 2023. 1, 3
- [26] Yuan Liu, Cheng Lin, Zijiao Zeng, Xiaoxiao Long, Lingjie Liu, Taku Komura, and Wenping Wang. Syncdreamer: Learning to generate multiview-consistent images from a single-view image. *arXiv preprint arXiv:2309.03453*, 2023. 3
- [27] Jonathan Lorraine, Kevin Xie, Xiao-hui Zeng, Chen-Hsuan Lin, Towaki Takikawa, Nicholas Sharp, Tsung-Yi Lin, Ming-Yu Liu, Sanja Fidler, and James Lucas. Att3d: Amortized text-to-3d object synthesis. *arXiv preprint arXiv:2306.07349*, 2023. 1
- [28] Luke Melas-Kyriazi, Iro Laina, Christian Rupprecht, and Andrea Vedaldi. Realfusion: 360deg reconstruction of any object from a single image. In *Proceedings of the IEEE/CVF Conference on Computer Vision and Pattern Recognition (CVPR)*, pages 8446–8455, 2023. 3
- [29] Ben Mildenhall, Pratul P. Srinivasan, Matthew Tancik, Jonathan T. Barron, Ravi Ramamoorthi, and Ren Ng. Nerf: Representing scenes as neural radiance fields for view synthesis. In *ECCV*, 2020. 3
- [30] Thomas Müller, Alex Evans, Christoph Schied, and Alexander Keller. Instant neural graphics primitives with a multiresolution hash encoding. *ACM Transactions on Graphics (ToG)*, 41(4):1–15, 2022. 3
- [31] Phong Nguyen-Ha, Nikolaos Sarafianos, Christoph Lassner, Janne Heikkilä, and Tony Tung. Free-viewpoint rgb-d human performance capture and rendering. In *European Conference on Computer Vision*, pages 473–491. Springer, 2022. 3
- [32] OpenAI. Gpt-4 technical report. *ArXiv*, abs/2303.08774, 2023. 6, 7
- [33] Ben Poole, Ajay Jain, Jonathan T. Barron, and Ben Mildenhall. Dreamfusion: Text-to-3d using 2d diffusion. In *The Eleventh International Conference on Learning Representations*, 2023. 1, 3, 4, 6
- [34] Alec Radford, Jong Wook Kim, Chris Hallacy, Aditya Ramesh, Gabriel Goh, Sandhini Agarwal, Girish Sastry, Amanda Askell, Pamela Mishkin, Jack Clark, Gretchen Krueger, and Ilya Sutskever. Learning transferable visual models from natural language supervision. In *Proceedings of the 38th International Conference on Machine Learning*, pages 8748–8763. PMLR, 2021. 3
- [35] Amit Raj, Srinivas Kaza, Ben Poole, Michael Niemeyer, Ben Mildenhall, Nataniel Ruiz, Shiran Zada, Kfir Aberman, Michael Rubenstein, Jonathan Barron, Yuanzhen Li, and Varun Jampani. Dreambooth3d: Subject-driven text-to-3d generation. *ICCV*, 2023. 1
- [36] Aditya Ramesh, Mikhail Pavlov, Gabriel Goh, Scott Gray, Chelsea Voss, Alec Radford, Mark Chen, and Ilya Sutskever. Zero-shot text-to-image generation. In *Proceedings of the 38th International Conference on Machine Learning*, pages 8821–8831. PMLR, 2021. 3
- [37] Jeremy Reizenstein, Roman Shapovalov, Philipp Henzler, Luca Sbordone, Patrick Labatut, and David Novotny. Common objects in 3d: Large-scale learning and evaluation of real-life 3d category reconstruction. In *International Conference on Computer Vision*, 2021. 3
- [38] Robin Rombach, Andreas Blattmann, Dominik Lorenz, Patrick Esser, and Björn Ommer. High-resolution image synthesis with latent diffusion models. In *CVPR*, 2022. 3, 5
- [39] Nataniel Ruiz, Yuanzhen Li, Varun Jampani, Yael Pritch, Michael Rubenstein, and Kfir Aberman. Dreambooth: Fine tuning text-to-image diffusion models for subject-driven generation. In *CVPR*, 2023. 3, 5
- [40] Chitwan Saharia, William Chan, Saurabh Saxena, Lala Li, Jay Whang, Emily Denton, Seyed Kamyar Seyed Ghasemipour, Raphael Gontijo-Lopes, Burcu Karagol Ayan, Tim Salimans, Jonathan Ho, David J. Fleet, and Mohammad Norouzi. Photorealistic text-to-image diffusion models with deep language understanding. In *Advances in Neural Information Processing Systems*, 2022. 3
- [41] Axel Sauer, Tero Karras, Samuli Laine, Andreas Geiger, and Timo Aila. StyleGAN-t: Unlocking the power of GANs for fast large-scale text-to-image synthesis. In *Proceedings of the 40th International Conference on Machine Learning*, pages 30105–30118. PMLR, 2023. 3
- [42] Zhan Shi, Xu Zhou, Xipeng Qiu, and Xiaodan Zhu. Improving image captioning with better use of caption. In *Proceedings of the 58th Annual Meeting of the Association for Computational Linguistics*, pages 7454–7464, 2020. 3
- [43] Zifan Shi, Sida Peng, Yinghao Xu, Andreas Geiger, Yiyi Liao, and Yujun Shen. Deep generative models on 3d representations: A survey. *arXiv preprint arXiv:2210.15663*, 2023. 1
- [44] Cheng Sun, Min Sun, and Hwann-Tzong Chen. Direct voxel grid optimization: Super-fast convergence for radiance fields reconstruction. In *Proceedings of the IEEE/CVF Conference on Computer Vision and Pattern Recognition*, pages 5459–5469, 2022. 3
- [45] Jiaxiang Tang, Jiawei Ren, Hang Zhou, Ziwei Liu, and Gang Zeng. Dreamgaussian: Generative gaussian splatting for efficient 3d content creation. *arXiv preprint arXiv:2309.16653*, 2023. 3
- [46] Ayush Tewari, Justus Thies, Ben Mildenhall, Pratul Srinivasan, Edgar Tretschk, Wang Yifan, Christoph Lassner, Vincent Sitzmann, Ricardo Martin-Brualla, Stephen Lombardi,

- et al. Advances in neural rendering. In *Computer Graphics Forum*, pages 703–735. Wiley Online Library, 2022. 3
- [47] Zhengyi Wang, Cheng Lu, Yikai Wang, Fan Bao, Chongxuan Li, Hang Su, and Jun Zhu. Prolificdreamer: High-fidelity and diverse text-to-3d generation with variational score distillation. *NeurIPS*, 2023. 1, 2, 3, 4, 5, 6, 7, 8
- [48] Haohan Weng, Tianyu Yang, Jianan Wang, Yu Li, Tong Zhang, CL Chen, and Lei Zhang. Consistent123: Improve consistency for one image to 3d object synthesis. *arXiv preprint arXiv:2310.08092*, 2023. 3
- [49] Olivia Wiles, Georgia Gkioxari, Richard Szeliski, and Justin Johnson. Synsin: End-to-end view synthesis from a single image. In *Proceedings of the IEEE/CVF Conference on Computer Vision and Pattern Recognition*, pages 7467–7477, 2020. 3
- [50] DeJia Xu, Yifan Jiang, Peihao Wang, Zhiwen Fan, Yi Wang, and Zhangyang Wang. Neurallift-360: Lifting an in-the-wild 2d photo to a 3d object with 360deg views. In *Proceedings of the IEEE/CVF Conference on Computer Vision and Pattern Recognition (CVPR)*, pages 4479–4489, 2023. 3
- [51] Alex Yu, Ruilong Li, Matthew Tancik, Hao Li, Ren Ng, and Angjoo Kanazawa. Plenotrees for real-time rendering of neural radiance fields. In *Proceedings of the IEEE/CVF International Conference on Computer Vision*, pages 5752–5761, 2021. 3
- [52] Jiahui Yu, Yuanzhong Xu, Jing Yu Koh, Thang Luong, Guncan Baid, Zirui Wang, Vijay Vasudevan, Alexander Ku, Yinfei Yang, Burcu Karagol Ayan, Ben Hutchinson, Wei Han, Zarana Parekh, Xin Li, Han Zhang, Jason Baldridge, and Yonghui Wu. Scaling autoregressive models for content-rich text-to-image generation. *Transactions on Machine Learning Research*, 2022. Featured Certification. 3
- [53] Hao Zhang, Feng Li, Shilong Liu, Lei Zhang, Hang Su, Jun Zhu, Lionel Ni, and Heung-Yeung Shum. DINO: DETR with improved denoising anchor boxes for end-to-end object detection. In *The Eleventh International Conference on Learning Representations*, 2023. 6